

# Band structure engineering of multinary chalcogenide topological insulators

Shiyong Chen,<sup>1,2</sup> X. G. Gong,<sup>2</sup> Chun-Gang Duan,<sup>1</sup> Zi-Qiang Zhu,<sup>1</sup> Jun-Hao Chu,<sup>1</sup> Aron Walsh,<sup>3</sup> Yu-Gui Yao,<sup>4</sup> Jie Ma,<sup>5</sup> and Su-Huai Wei<sup>5</sup>

<sup>1</sup>Laboratory of Polar Materials and Devices, East China Normal University, Shanghai 200241, China

<sup>2</sup>Laboratory for Computational Physical Sciences and Surface Physics Laboratory, Fudan University, Shanghai 200433, China

<sup>3</sup>Department of Chemistry, University College London, London WC1E 6BT, United Kingdom

<sup>4</sup>Institute Of Physics, Chinese Academy of Sciences, Beijing 100190, China

<sup>5</sup>National Renewable Energy Laboratory, Golden, Colorado 80401, USA

(Received 25 March 2011; revised manuscript received 10 May 2011; published 17 June 2011)

Topological insulators (TIs) have been found in strained binary HgTe and ternary I-III-VI<sub>2</sub> chalcopyrite compounds such as CuTiSe<sub>2</sub> which have inverted band structures. However, the nontrivial band gaps of these existing binary and ternary TIs are limited to small values, usually around 10 meV or less. In this work, we reveal that a large nontrivial band gap requires the material to have a large negative crystal field splitting  $\Delta_{CF}$  at the top of the valence band and a moderately large negative  $s$ - $p$  band gap  $E_g^{s-p}$ . These parameters can be better tuned through chemical ordering in multinary compounds. Based on this understanding, we show that a series of quaternary I<sub>2</sub>-II-IV-VI<sub>4</sub> compounds, including Cu<sub>2</sub>HgPbSe<sub>4</sub>, Cu<sub>2</sub>CdPbSe<sub>4</sub>, Ag<sub>2</sub>HgPbSe<sub>4</sub>, and Ag<sub>2</sub>CdPbTe<sub>4</sub>, are TIs, in which Ag<sub>2</sub>HgPbSe<sub>4</sub> has the largest TI band gap of 47 meV because it combines the optimal values of  $\Delta_{CF}$  and  $E_g^{s-p}$ .

DOI: 10.1103/PhysRevB.83.245202

PACS number(s): 73.20.At, 71.15.Dx, 71.18.+y, 73.61.Le

## I. INTRODUCTION

The search for new topological insulators (TIs) has intensified recently due to their scientific importance as representing a novel quantum state and the associated technological applications in spintronics and quantum computing.<sup>1,2</sup> So far, experimental realizations have been limited to a few classes of simple materials, including zinc-blende-based HgTe quantum wells,<sup>3-5</sup> Bi<sub>1-x</sub>Sb<sub>x</sub> alloys,<sup>6,7</sup> and binary tetradymite semiconductors such as Bi<sub>2</sub>Se<sub>3</sub> and Bi<sub>2</sub>Te<sub>3</sub>.<sup>8-10</sup> Most recently, the search for TIs has extended to ternary compounds,<sup>11-14</sup> e.g., strained half-Heusler compounds, in the hope that the presence of more chemical elements would bring greater material flexibility. Despite the success in identifying these TIs, the design of new TI materials with the following advantages is still desired: (i) realization of a topological insulating state with a significant nontrivial band gap (i.e., larger than  $kT$  at room temperature) in its natural equilibrium state (i.e., not under external strain), (ii) easy integration with electronic and spintronic devices based on tetrahedral semiconductors, and (iii) ease of synthesis or already synthesized.

Based on the direct evaluation of the  $Z_2$  topological invariant, Feng *et al.*<sup>15</sup> proposed that a series of I-III-VI<sub>2</sub> chalcopyrite compounds (such as CuTiSe<sub>2</sub>) could have topologically nontrivial band structure, and some of them can realize a topological insulating phase in their natural equilibrium structure. This is an important observation because the chalcopyrite structure is derived from the zinc-blende structure, and the band structure properties are well understood, mostly for solar cell applications.<sup>16,17</sup> Some of the proposed Cu- and Ag-based TIs, such as CuTiSe<sub>2</sub> and AgTiTe<sub>2</sub>, have already been synthesized experimentally.<sup>16,18</sup> However, the predicted band gaps of these TIs are very small, usually around 10 meV or less, similar to that observed in strained HgTe.<sup>4</sup>

In this paper, we show that the nontrivial band gaps of zinc-blende-derived compounds with inverted band structure are mainly determined by the crystal field splitting  $\Delta_{CF}$  at the

top of the valence band and the size of the inverted  $s$ - $p$  band gap  $E_g^{s-p}$ , which can be better tuned by changing the component elements in a multinary ordered compounds. A large nontrivial band gap requires the material to have a large negative  $\Delta_{CF}$  and a large negative  $E_g^{s-p}$  as long as it has no band crossing at the Fermi energy. For I-III-VI<sub>2</sub> topological insulators, because the band inversion requires the group-III elements to be large and heavy, whereas a large negative  $\Delta_{CF}$  requires group-III elements to be small and light, the possibilities for obtaining a large TI band gap are limited. Through further cation mutation, large negative  $\Delta_{CF}$  and  $E_g^{s-p}$  are achievable in quaternary II<sub>2</sub>-II-IV-VI<sub>4</sub> compounds. We have identified four topological insulators (Cu<sub>2</sub>HgPbSe<sub>4</sub>, Cu<sub>2</sub>CdPbSe<sub>4</sub>, Ag<sub>2</sub>HgPbSe<sub>4</sub>, and Ag<sub>2</sub>CdPbTe<sub>4</sub>), in which Ag<sub>2</sub>HgPbSe<sub>4</sub> has the largest TI band gap of 47 meV. In the following, we will discuss the evolution of the band structure of zinc-blende-derived structures first, explain what kind of band structure can lead to the largest TI band gap, and then show how to design quaternary TIs through cation mutation.

## II. CALCULATION METHODS

The band structures are calculated within the density functional theory (DFT) formalism as implemented in the VASP code.<sup>19</sup> For the exchange-correlation functional, we used the Heyd-Scuseria-Ernzerhof (HSE) hybrid functional in which one-quarter of the Hartree-Fock nonlocal exchange interaction is added to the generalized gradient approximation (GGA) functional, and a screening of  $\mu = 0.2 \text{ \AA}^{-1}$  is applied to partition the exchange potential into short-range and long-range terms.<sup>20-22</sup> The  $d$  states of group-III and -IV elements are treated explicitly as valence states. The interaction between the core electrons and the valence electrons is included by the frozen-core projector augmented-wave method, and an energy cutoff of 300 eV was applied for the plane-wave basis set. A  $4 \times 4 \times 4$  Monkhorst-Pack  $k$ -point mesh is used for the Brillouin-zone integration of the eight-atom chalcopyrite and

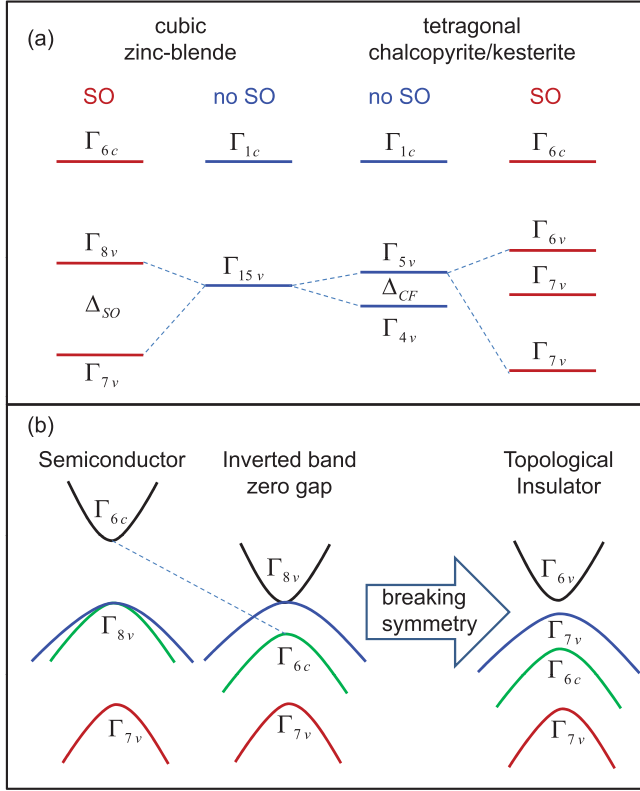


FIG. 1. (Color online) (a) The conduction and valence band splitting of cubic and tetragonal semiconductors. (b) A plot showing how the band structure of normal semiconductors transfers into the inverted and topological insulator band structures. Note that the subscript  $v$  (c) represents that the state belongs to the valence (conduction) band in the normal band structure.

kesterite cells. All lattice vectors and atomic positions were fully relaxed.

### III. FACTORS DETERMINING THE NONTRIVIAL BAND GAP

For normal zinc-blende semiconductors such as CdTe, the band gap is between the  $s$ -like conduction band minimum (CBM)  $\Gamma_{6c}$  state and the  $p$ -like valence band maximum (VBM)  $\Gamma_{8v}$  state, as shown in Fig. 1. The nontrivial band structure of a TI is characterized by band inversion in the Brillouin zone,<sup>6,15</sup> i.e., the position of the conduction and valence bands is switched. In zinc-blende compounds, the band inversion means that the  $\Gamma_{6c}$  level falls below the  $\Gamma_{8v}$  level. In the inverted band structure, the  $\Gamma_{6c}$  level is occupied, while the quadruply degenerate  $\Gamma_{8v}$  level is half occupied, making the Fermi level stay at the  $\Gamma_{8v}$  level and the system become a zero-gap semimetal. This is the case for bulk HgTe.

To open a band gap and change the zinc-blende semimetal HgTe into a topological insulator, one has to induce a crystal field splitting  $\Delta_{CF}$  by reducing the  $T_d$  symmetry of the zinc-blende structure to, e.g.,  $D_{2d}$ , by applying an epitaxial strain or forming a quantum well.<sup>4</sup> For  $D_{2d}$  symmetry, the half-filled  $\Gamma_{8v}$  state splits into  $\Gamma_{6v}$  and  $\Gamma_{7v}$  states, and a gap can be opened around the occupied  $\Gamma_{7v}$  ( $\Gamma_{6v}$ ) and unoccupied  $\Gamma_{6v}$  ( $\Gamma_{7v}$ ) levels [Fig. 1(b)] if  $\Delta_{CF}$  is positive (negative). On the other hand,

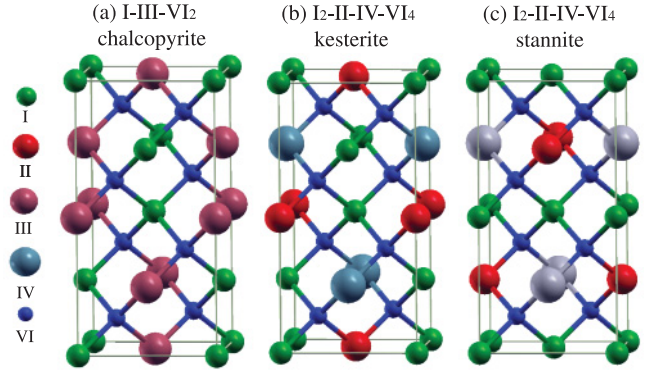


FIG. 2. (Color online) Crystal structure plot of (a) ternary I-III-VI<sub>2</sub> chalcopyrite structure, (b) quaternary I<sub>2</sub>-II-IV-VI<sub>4</sub> kesterite structure, and (c) quaternary I<sub>2</sub>-II-IV-VI<sub>4</sub> stannite structure.

the crystal field splitting can also be induced by chemical ordering, e.g., by mutating two Hg (group-II) atoms into one Cu (group I) and one Tl (group III), forming ordered I-III-VI<sub>2</sub> chalcopyrite-structured compounds such as CuTlTe<sub>2</sub>.<sup>15</sup> In Fig. 2(a) we plot the chalcopyrite structure, which can be taken as derived from the binary zinc-blende structure.<sup>23,24</sup>

In Fig. 3 we plot the calculated band structure of HgTe under an  $\epsilon = 0.02$  (001) tensile strain with  $\Delta_{CF} = 70$  meV and CuTlTe<sub>2</sub> in the chalcopyrite structure with  $\Delta_{CF} = 76$  meV. As we can see, a small gap is opened near the  $\Gamma$  point for both systems, which is the so-called nontrivial band gap of TIs. Although the size is small, this anticrossing gap is protected by the lattice symmetry.<sup>25</sup> For the band structure calculation we employed density functional theory with a hybrid exchange-correlation functional (HSE),<sup>20</sup> which can more correctly predict the band gaps of many zinc-blende and chalcopyrite semiconductors.<sup>21,22,26</sup> However, it should be mentioned that, due to the similar wave-function characters of the band edge states and symmetry-protected nature of the TI band gap, the TI band gap does not disappear even in the calculated band structure using the local density approximation (LDA) to the exchange correlation functional, even though the LDA usually underestimates the  $s$ - $p$  band gap significantly.

Comparing the band structure of HgTe under an  $\epsilon = 0.02$  (001) tensile strain and that of CuTlTe<sub>2</sub>, we find that the overall shape is very similar, especially near the band gap. In both systems, the  $s$ -like  $\Gamma_{6c}$  state falls below the  $p$ -like  $\Gamma_{6v}$  and  $\Gamma_{7v}$  states, and the minimum gap occurs along the  $\Gamma$ - $X$  line. This similarity between strained HgTe and CuTlTe<sub>2</sub> indicates that the strain and chemical ordering have the same effect in producing the crystal field splitting  $\Delta_{CF}$  at the top of the valence band;<sup>27</sup> therefore, chemical ordering could be an efficient way to tune the TI band gap.

To achieve this goal, it is important to understand first how the splitting at the top of valence band is influenced by chemical ordering and what is the resulting dependence of the TI band gap. Based on the quasicubic model,<sup>27,28</sup> and assuming the  $\Gamma_{6c}$  state is far away from the band edge, we know that the splitting of the  $\Gamma_{8v}$  level into  $\Gamma_{6v}$  and  $\Gamma_{7v}$  under the tetragonal symmetry depends on two quantities: the spin-orbit splitting  $\Delta_{SO}$  and the crystal field splitting  $\Delta_{CF}$ .  $\Delta_{CF}$  is defined to be positive if the doubly degenerate  $\Gamma_{5v}$  is above the singly degenerate  $\Gamma_{4v}$  state when the spin-orbit

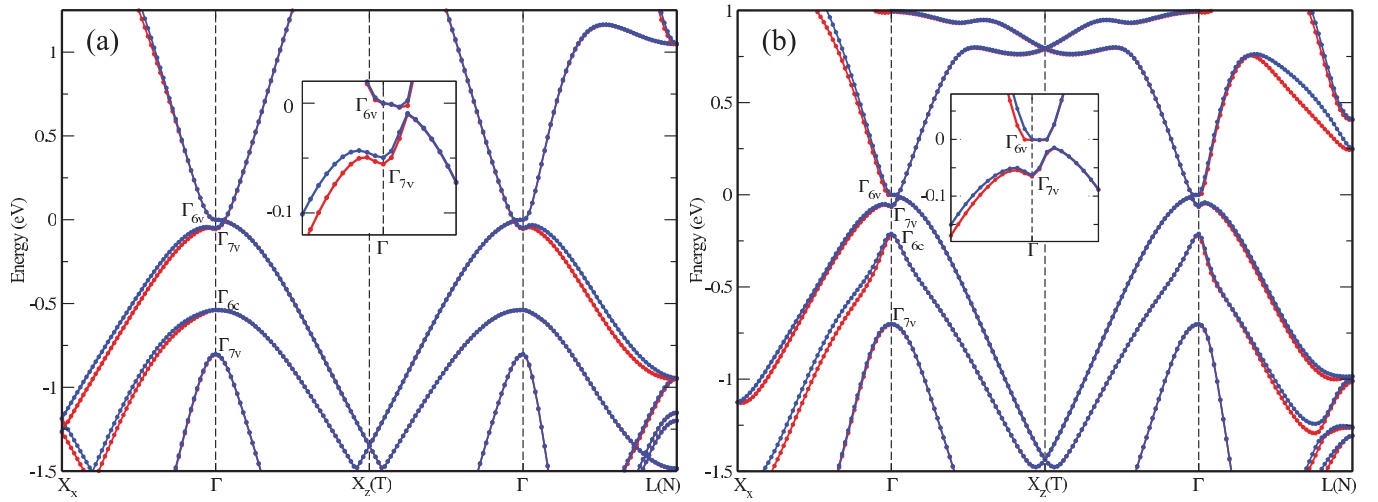


FIG. 3. (Color online) The calculated band structure along the high-symmetry lines  $X_X: \frac{2\pi}{a}(100) \rightarrow \Gamma:(000) \rightarrow X_Z: \frac{2\pi}{a}(001) \rightarrow \Gamma:(000) \rightarrow L: \frac{2\pi}{a}(0.50.50.5)$  of (a) HgTe with a (001) tensile strain and  $\Delta_{CF} = 70$  meV, and (b) CuTlTe<sub>2</sub> with  $\Delta_{CF} = 76$  meV at its equilibrium state.  $X_X$ ,  $X_Z$ , and  $L$  are the notations for the zinc-blende structure, and  $X_Z$  and  $L$  correspond to  $T$  and  $N$ , respectively, in the chalcopyrite structure. Red and blue colors are used to show the two spin-dependent bands clearly.

interaction is not considered, as shown in Fig. 1(a). For systems where  $\Delta_{SO}$  is much larger than  $\Delta_{CF}$ , the splitting between  $\Gamma_{6v}$  and  $\Gamma_{7v}$  is close to  $2/3$  of  $\Delta_{CF}$ . Previous studies<sup>25</sup> on strained zinc-blende compound showed that the nontrivial gap depends on the sign and size of  $\Delta_{CF}$ : (i) when  $\Delta_{CF} < 0$  the gap occurs along the  $\Gamma$ - $X_X$  line near the  $\Gamma$  point and the gap increases quickly as a function of the magnitude of  $\Delta_{CF}$ ; (ii) when  $\Delta_{CF} > 0$ , the gap occurs along the  $\Gamma$ - $X_Z$  line near the  $\Gamma$  point and the gap increases slowly as a function of  $\Delta_{CF}$ . This can be seen clearly in Fig. 4(a), where the dependence of the nontrivial band gap on the size of  $\Delta_{CF}$  for HgTe is plotted. For example, when  $\Delta_{CF} = -100$  meV, the gap is almost 40 meV, but when  $\Delta_{CF} = 100$  meV, the gap is only 5 meV. The reason for the more significant gap increase with negative  $\Delta_{CF}$  is that the  $\Gamma$ - $X_X$  line has lower symmetry than the  $\Gamma$ - $X_Z$  line, so the band anticrossing is more significant when the gap shifts to the  $\Gamma$ - $X_X$  line. CuTlTe<sub>2</sub> has a calculated  $\Delta_{CF} = 76$  meV. This positive value explains why the gap shifts to the  $\Gamma$ - $X_Z$  line

with only a small value of about 14 meV [Fig. 3(b)]. Based on this observation, we know that a large-gap TI can only exist in zinc-blende-derived compounds with large negative  $\Delta_{CF}$ .

In Fig. 4(b) we plot the calculated  $\Delta_{CF}$  of CuAlTe<sub>2</sub>, CuGaTe<sub>2</sub>, CuInTe<sub>2</sub>, and CuTlTe<sub>2</sub>. As we can see,  $\Delta_{CF}$  increases from negative to positive as the group-III cations change from Al to Tl, i.e., from small light to large heavy elements. Considering that large negative  $\Delta_{CF}$  enlarges the nontrivial gap, one may intend to search for compounds with small group-III cations as candidates for TIs. However, the requirement of band inversion at the  $\Gamma$  point excludes Al, Ga, and In compounds because CuAlTe<sub>2</sub>, CuGaTe<sub>2</sub>, and CuInTe<sub>2</sub> all have the normal band order, i.e., the  $s$ -like  $\Gamma_{6c}$  state is above the  $p$ -like  $\Gamma_{7v}$  and  $\Gamma_{6v}$  states. Their  $s$ - $p$  band gaps  $E_g^{s-p} = E(\Gamma_{6c}) - E(\Gamma_{6,7v})$  are all positive and decrease from Al to Ga to In compounds. This can be understood according to the band component of I-III-VI<sub>2</sub> chalcopyrites: the  $\Gamma_{6c}$  state has  $s$ -like antibonding character localized on the group-III cation and the group-VI anion, whereas  $\Gamma_{7v}$  and  $\Gamma_{6v}$  states mainly have the  $p$  component of the group-VI anion hybridized with the  $d$  component of the group-I cation.<sup>29,30</sup> Two factors shift the  $\Gamma_{6c}$  level down from Al to Ga to In compounds:<sup>17,23,30</sup> (i) the  $s$  orbital energy of Ga is deeper than that of Al and (ii) In is much larger than Ga. For Tl, its  $s$  orbital energy, like Hg, is very deep due to the large relativistic effect, so its band gap is much lower than that of the corresponding In compounds. This is confirmed in Fig. 4(c), where we plot the calculated  $E_g^{s-p}$  of CuAlTe<sub>2</sub>, CuGaTe<sub>2</sub>, CuInTe<sub>2</sub>, and CuTlTe<sub>2</sub>; only CuTlTe<sub>2</sub> has negative  $E_g^{s-p}$ , i.e., its  $s$ -like  $\Gamma_{6c}$  state falls below the  $p$ -like states at the  $\Gamma$  point (band inversion). Unfortunately, CuTlTe<sub>2</sub> has a positive  $\Delta_{CF} = 76$  meV and thus only a small TI band gap of about 14 meV.

In the above discussion, we have assumed that the  $\Gamma_{6c}$  state is deep inside the valence band and thus has no effect on the band splitting and the nontrivial gap of the TIs. However, if the  $\Gamma_{6c}$  is close to the band edge, then we have to consider its interaction with the band edge states.

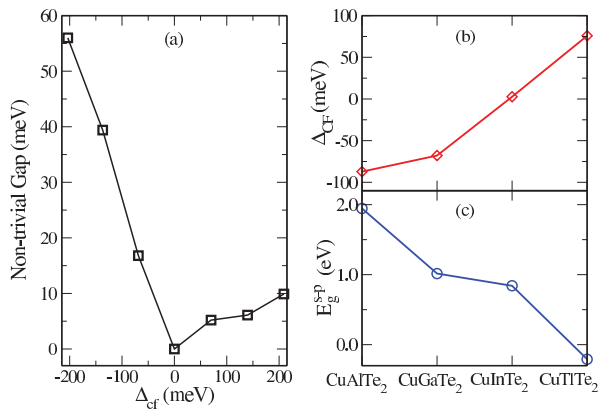


FIG. 4. (Color online) (a) The calculated nontrivial band gap as a function of  $\Delta_{CF}$  for HgTe. Here  $\Delta_{CF}$  is changed by tuning the (001) strain  $\epsilon$ . (b) The calculated  $\Delta_{CF}$  and (c)  $E_g^{s-p}$  of Cu-III-Te<sub>2</sub> with III Al, Ga, In, or Tl.

This is because when  $\Delta_{CF} < 0$ , the band gap of the TI at the  $\Gamma$  point is between the unoccupied  $\Gamma_{7v}$  and the occupied  $\Gamma_{6v}$  (or  $\Gamma_{6c}$ , if it has a higher energy than  $\Gamma_{6v}$ ) derived states. The coupling between the  $\Gamma_{6v}$  and  $\Gamma_{6c}$  states pushes the  $\Gamma_{6v}$  level up in energy, thus reducing the effective crystal field splitting between the  $\Gamma_{7v}$  and  $\Gamma_{6v}$  states and the nontrivial band gap. This is what we find for  $\text{AgTlSe}_2$  and  $\text{AgTlTe}_2$ . According to our calculation, the nontrivial gap of  $\text{AgTlSe}_2$  is limited at the  $\Gamma$  point, with a very small size, 1 meV, although it has a large negative  $\Delta_{CF} = -50$  meV. Therefore, to reduce the interaction between the  $\Gamma_{6v}$  and  $\Gamma_{6c}$  states, one should move the  $\Gamma_{6c}$  level down, i.e., increase the magnitude of the negative  $E_g^{s-p}$  as much as possible.

The above analysis indicates that to design large-gap chalcopyrite I-III-VI<sub>2</sub> TIs, we face two contradictory requirements (large negative  $\Delta_{CF}$  and large negative  $E_g^{s-p}$ ). This severely limits the largest nontrivial gap obtainable for I-III-VI<sub>2</sub> compounds. Through a direct calculation, we find that most of the already synthesized I-III-VI<sub>2</sub> compounds have positive  $E_g^{s-p}$  and are normal semiconductors,<sup>16</sup> except for  $\text{CuTlSe}_2$ ,  $\text{CuTlTe}_2$ ,  $\text{AgTlSe}_2$ , and  $\text{AgTlTe}_2$ . But the nontrivial gaps of these four TIs are all small due to the positive  $\Delta_{CF}$  for  $\text{CuTlSe}_2$  and  $\text{CuTlTe}_2$  and small  $E_g^{s-p}$  for  $\text{AgTlSe}_2$  and  $\text{AgTlTe}_2$ .

#### IV. QUATERNARY TOPOLOGICAL INSULATORS

To further increase the nontrivial band gap, we need to make both  $\Delta_{CF}$  and  $E_g^{s-p}$  more negative. We find that this can be done by mutating two group-III cations in I-III-VI<sub>2</sub> compounds to one group-II and one group-IV cation, thus forming the I<sub>2</sub>-II-IV-VI<sub>4</sub> (I = Cu, Ag, II = Zn, Cd, Hg, IV = Si, Ge, Sn, Pb, VI = S, Se, Te) quaternary compounds. These compounds crystallize in either tetrahedral kesterite or stannite structures, as shown in Figs. 2(b) and 2(c). Due to the increased chemical and structural freedom in the quaternary compounds, their band structures can be better tuned. Also, because they are structurally derived from chalcopyrites, their band structures

TABLE I. The calculated  $E_g^{s-p}$  of I<sub>2</sub>-II-Pb-VI<sub>4</sub> (I = Cu, Ag, II = Cd, Hg, VI = S, Se, Te) in their ground-state structures. TM, TI, and NI in parentheses represent topological metal, topological insulator, and normal insulator, respectively.

	Structure	Te <sub>4</sub>	Se <sub>4</sub>	S <sub>4</sub>
Cu <sub>2</sub> HgPb	Stannite	-0.46 (TM)	-0.32 (TI)	0.07 (NI)
Cu <sub>2</sub> CdPb	Stannite	-0.21 (TM)	-0.07 (TI)	0.32 (NI)
Ag <sub>2</sub> HgPb	Kesterite	-0.37 (TM)	-0.14 (TI)	0.40 (NI)
Ag <sub>2</sub> CdPb	Kesterite	-0.12 (TI)	0.18 (NI)	0.72 (NI)

maintain similar characteristics to those of chalcopyrites;<sup>23,24</sup> therefore, the empirical rule that if the  $s$ -orbital-originated  $\Gamma_{6c}$  state is completely occupied and below the valence band maximum the compound possesses a nontrivial topological band structure given by Feng *et al.* for the chalcopyrites is also valid for the quaternary compounds,<sup>15</sup> i.e., if these compounds have inverted band structure, they can also be TIs.

As for the chalcopyrites, we need to have compounds that contain heavy group-IV elements so that the  $\Gamma_{6c}$  level could fall below the  $\Gamma_{6v}$  and  $\Gamma_{7v}$  levels.<sup>23,24</sup> Table I lists the calculated  $E_g^{s-p}$  of I<sub>2</sub>-II-Pb-VI<sub>4</sub> compounds. The results show that most of the Pb-Te and Pb-Se compounds have negative  $E_g^{s-p}$  at  $\Gamma$  and are therefore candidates for TIs. The calculation also shows that all sulfides and compounds containing other group-IV cations (Sn, Ge, Si) have positive  $E_g^{s-p}$  and are normal semiconductors.

We first look at the band structure of  $\text{Cu}_2\text{HgPbTe}_4$  [Fig. 5(a)], which has the most negative  $E_g^{s-p}$ . The overall shape near the  $\Gamma$  point is similar to those of ternary  $\text{CuTlTe}_2$  and binary  $\text{HgTe}$  under (001) strain as shown in Fig. 3, indicating that the band structure character is retained in the cation mutation. However,  $\text{Cu}_2\text{HgPbTe}_4$  is actually a topological metal (TM), because the conduction band near the  $L(N)$ :  $\frac{2\pi}{a}$  (0.50.50.5) point drops below the VBM and crosses the Fermi level [see Fig. 5(a)]. The reason is that the conduction band state at the  $L(N)$  point has similar character to the  $\Gamma_{6c}$

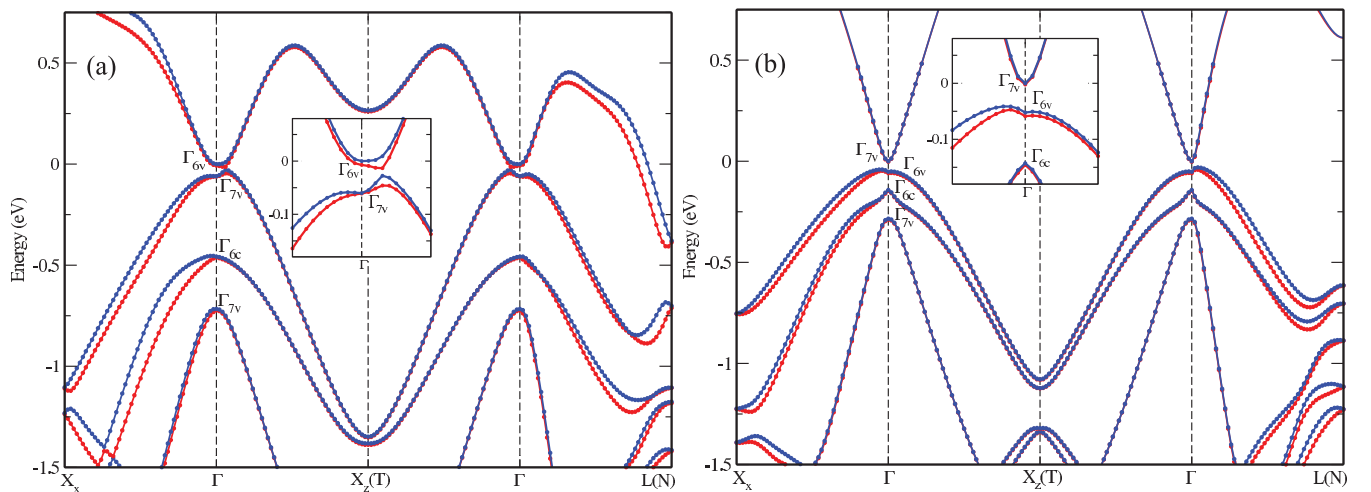


FIG. 5. (Color online) The calculated band structure along the high-symmetry lines  $X_X \rightarrow \Gamma \rightarrow X_Z(T) \rightarrow \Gamma \rightarrow L(N)$  of (a)  $\text{Cu}_2\text{HgPbTe}_4$  and (b)  $\text{Ag}_2\text{HgPbSe}_4$  in their equilibrium states.



state, so when the  $\Gamma_{6c}$  energy is too low, the  $L_{1c}(N_{1c})$  state energy is also below the VBM, making the system metallic. To avoid this situation, therefore, we should search for a TI material with mildly negative  $E_g^{s-p}$ .

Our previous study<sup>23,30</sup> has shown that replacing Cu by Ag or replacing Te by Se can increase  $E_g^{s-p}$ , i.e., raising the  $\Gamma_{6c}$  and  $L_{1c}$  energy levels relative to  $\Gamma_{6v}$  and  $\Gamma_{7v}$ , because (i) at the top of the valence band, the lower  $4d$  level and larger size of Ag compared to Cu weaken the  $p$ - $d$  hybridization, and the  $4p$  level of Se is lower than the  $5p$  level of Te, which both shift the  $\Gamma_{6v}$  and  $\Gamma_{7v}$  levels down; (ii) the displacement of the anion toward Pb in the Ag compounds and the smaller size of Se than Te also both reduce the Pb-anion bond lengths, increasing the energy of the Pb(s)-anion(s) antibonding states at the bottom of the conduction band. This expectation is supported by the calculated band structure of  $\text{Ag}_2\text{HgPbSe}_4$ , which has no band crossing at the Fermi level; thus this compound is a topological insulator, as shown in Fig. 5(b). Similarly, we predict that  $\text{Cu}_2\text{CdPbTe}_4$  and  $\text{Ag}_2\text{HgPbTe}_4$  are topological metals, while  $\text{Cu}_2\text{HgPbSe}_4$ ,  $\text{Cu}_2\text{CdPbSe}_4$ , and  $\text{Ag}_2\text{CdPbTe}_4$  are topological insulators. The results are shown in Table I.

Among the four identified quaternary TIs,  $\text{Ag}_2\text{HgPbSe}_4$  has the largest nontrivial gap of 47 meV. This is because  $\text{Ag}_2\text{HgPbSe}_4$  is more stable in the low-symmetry kesterite structure with a large group-I element; therefore, it has a large negative  $\Delta_{CF}$  (−51 meV). It also has a reasonably large negative  $E_g^{s-p}$  gap, so the coupling between the  $\Gamma_{6c}$  and the  $\Gamma_{6v}$  states is weak. Its band structure is shown in Fig. 5(b). As expected, we see that the gap of  $\text{Ag}_2\text{HgPbSe}_4$  occurs at a

position along the low-symmetry  $\Gamma$ - $X_X$  line, consistent with our discussion above.

## V. CONCLUSIONS

In conclusion, we have shown that the nontrivial band gaps of zinc-blende-derived topological insulators depend on the crystal field splitting at the top of the valence band as well as the size of the inverted  $s$ - $p$  band gap. In general, a material with large TI band gap should have a large negative crystal field splitting and a moderate size of the inverted band gap. Compared to binary zinc-blende and ternary chalcopyrite compounds, these parameters can be more easily tuned through the chemical ordering in quaternary compounds. Based on this understanding, we have identified four ground state quaternary topological insulators, among which  $\text{Ag}_2\text{HgPbSe}_4$  has the largest TI band gap of 47 meV because it has the optimal band structure parameters.

## ACKNOWLEDGMENTS

This work is supported by NSF of Shanghai (Grant No. 10ZR1408800) and China (Grants No. 10934002, No. 10950110324, and No. 10974231), the Research Program of Shanghai Municipality and MOE, the Special Funds for Major State Basic Research, the Fundamental Research Funds for the Central Universities, CC of ECNU, PCSIRT, and the 973 Program (Grant No. 2007CB924900). The work at NREL is funded by the US Department of Energy, under Contract No. DE-AC36-08GO28308.

<sup>1</sup>X. L. Qi and S. C. Zhang, *Phys. Today* **63**(1), 33 (2010).

<sup>2</sup>J. E. Moore, *Nature (London)* **464**, 194 (2010).

<sup>3</sup>M. König *et al.*, *Science* **318**, 766 (2007).

<sup>4</sup>B. A. Bernevig, T. L. Hughes, and S. C. Zhang, *Science* **314**, 1757 (2006).

<sup>5</sup>J. W. Luo and A. Zunger, *Phys. Rev. Lett.* **105**, 176805 (2010).

<sup>6</sup>L. Fu and C. L. Kane, *Phys. Rev. B* **76**, 045302 (2007).

<sup>7</sup>D. Hsieh *et al.*, *Nature (London)* **452**, 970 (2008); **323**, 919 (2009).

<sup>8</sup>Y. Xia *et al.*, *Nature Phys.* **5**, 398 (2009).

<sup>9</sup>Y. L. Chen *et al.*, *Science* **325**, 178 (2009).

<sup>10</sup>H. Zhang, C. X. Liu, X. L. Qi, X. Dai, Z. Fang, and S. C. Zhang, *Nature Phys.* **5**, 438 (2009).

<sup>11</sup>H. Lin *et al.*, *Nature Mater.* **9**, 546 (2010).

<sup>12</sup>D. Xiao, Y. Yao, W. Feng, J. Wen, W. Zhu, X. Q. Chen, G. M. Stocks, and Z. Zhang, *Phys. Rev. Lett.* **105**, 096404 (2010).

<sup>13</sup>S. Chadov, X. Qi, J. Kbler, G. H. Fecher, C. Felser, and S. C. Zhang, *Nature Mater.* **9**, 541 (2010).

<sup>14</sup>H. Lin, R. S. Markiewicz, L. A. Wray, L. Fu, M. Z. Hasan, and A. Bansil, *Phys. Rev. Lett.* **105**, 036404 (2010); B. Yan *et al.*, *Europhys. Lett.* **90**, 37002 (2010); Y. Chen *et al.*, *Phys. Rev. Lett.* **105**, 266401 (2010); T. Sato, K. Segawa, H. Guo, K. Sugawara, S. Souma, T. Takahashi, and Y. Ando, *ibid.* **105**, 136802 (2010).

<sup>15</sup>W. Feng, D. Xiao, J. Ding, and Y. Yao, *Phys. Rev. Lett.* **106**, 016402 (2011).

<sup>16</sup>O. M. Madelung, *Semiconductors: Data Handbook*, 3rd ed. (Springer, Berlin, 2004).

<sup>17</sup>S.-H. Wei and A. Zunger, *J. Appl. Phys.* **78**, 3846 (1995).

<sup>18</sup>M. Bohm, G. Huber, A. MacKinnon, O. Madelung, A. Scharmann, and E.-G. Scharmer, *Physics of Ternary Compounds* (Springer, New York, 1985).

<sup>19</sup>G. Kresse and J. Furthmüller, *Phys. Rev. B* **54**, 11169 (1996).

<sup>20</sup>J. Heyd, G. E. Scuseria, and M. Ernzerhof, *J. Chem. Phys.* **118**, 8207 (2003).

<sup>21</sup>J. Paier, M. Marsman, K. Hummer, G. Kresse, I. Gerber, and J. Angyan, *J. Chem. Phys.* **124**, 154709 (2006).

<sup>22</sup>K. Hummer, A. Gruneis, and G. Kresse, *Phys. Rev. B* **75**, 195211 (2007).

<sup>23</sup>S. Chen, X. G. Gong, A. Walsh, and S.-H. Wei, *Phys. Rev. B* **79**, 165211 (2009).

<sup>24</sup>S. Chen, X. G. Gong, A. Walsh, and S.-H. Wei, *Appl. Phys. Lett.* **94**, 041903 (2009).

<sup>25</sup>C.-Y. Moon and S.-H. Wei, *Phys. Rev. B* **74**, 045205 (2006).

<sup>26</sup>J. Paier, R. Asahi, A. Nagoya, and G. Kresse, *Phys. Rev. B* **79**, 115126 (2009).

<sup>27</sup>S.-H. Wei and A. Zunger, *Phys. Rev. B* **49**, 14337 (1994).

<sup>28</sup>J. E. Rowe and J. L. Shay, *Phys. Rev. B* **3**, 451 (1971).

<sup>29</sup>J. E. Jaffe and A. Zunger, *Phys. Rev. B* **28**, 5822 (1983).

<sup>30</sup>S. Chen, X. G. Gong, and S.-H. Wei, *Phys. Rev. B* **75**, 205209 (2007).